The energy dependence of the centroid frequency and phase lag of the QPOs in GRS 1915+105

J. L. Qu[1], F. J. Lu[1], Y. Lu[1], L. M. Song[1], S. Zhang[1], G. Q. Ding[2]

Key Laboratory for Particle Astrophysics, Institute of High Energy Physics, CAS, Beijing, P. R. China

Received _____; accepted _____

Not to appear in Nonlearned J., 45.

[1]Key Laboratory for Particle Astrophysics, Institute of High Energy Physics, Chinese Academy of Sciences (CAS), 19B Yuquan Road, Beijing 100049, P. R. China; Email: qujl@ihep.ac.cn.

[2]Urumqi Observatory, NAOC, 40-5 South Beijing Road, Urumqi, Xinjiang 830011, P. R. China; Email: dinggq@uao.ac.cn

ABSTRACT

We present a study of the centroid frequencies and phase lags of the quasi-periodic oscillations (QPOs) as functions of photon energy for GRS 1915+105. It is found that the centroid frequencies of the 0.5-10 Hz QPOs and their phase lags are both energy dependent, and there exists an anti-correlation between the QPO frequency and phase lag. These new results challenge the popular QPO models, because none of them can fully explain the observed properties. We suggest that the observed QPO phase lags are partially due to the variation of the QPO frequency with energy, especially for those with frequency higher than 3.5 Hz.

Subject headings: accretion, accretion disks — black hole physics — stars: individual (GRS 1915+105) — stars: oscillations

1. Introduction

GRS 1915+105 is a low-mass X-ray black hole binary showing a rich diversity of X-ray lightcurve morphology and complex timing phenomena (Morgan et al. 1997; Cui 1999; Belloni et al. 2000; Ji et al. 2003). The variability of the source can be reduced to transitions between three basic states: a hard state corresponding to the non-observability of the innermost part of the accretion disk (state C), and two softer states with a fully observable disk but different temperatures (states B and A) (Belloni et al. 1997a,b; 2000). According to the appearance of light curves and color-color diagrams, the behaviors of the source can be further classified into 12 classes (Belloni et al. 2000). In additional to the above flux and spectral variabilities, abundant quasi-periodic oscillations (QPOs) are also observed in this system. The fundamental frequency of its QPO ranges from mHz to several hundred Hz, and some QPOs are detected up to the third harmonic (Morgan et al. 1997; Cui 1999). According to their (fundamental) frequencies, the QPOs of GRS 1915+105 can be divided into three classes: the low-frequency ($\sim$1-67 mHz) QPOs, the intermediate-frequency (0.5-10 Hz) QPOs, and the high-frequency ($\sim$ 67 Hz) QPOs. These QPOs occur in different states of the accretion disk of the source (Chakrabarti & Manickam 2000). The low-frequency QPOs and the high-frequency QPOs are often observed during the soft state of GRS 1915+105 (state B). The low-frequency QPOs are considered to be connected with disk instability, as the rapid disappearance and refill of the inner accretion disk (Belloni et al. 2000). The high-frequency QPO has been proposed to arise in the close vicinity of the black hole and been thought to reflect the general relativity properties of the black hole (Cui et al. 1998). Conversely, the intermediate-frequency QPOs only appear in state C of the source, and never appear in state B. Although it is suggested that the 0.5–2 Hz QPOs may originate from the compact jet (Fender 2005), the phase-resolved spectra and variation of the phase lags with frequencies show that the 0.5-10 Hz QPOs are all from the inner disk (Miller & Human, 2005; Reig et al. 2001). They are linked to

the properties of the accretion disk since their centroid frequencies and fractional rms are correlated with the thermal flux and the apparent temperature of the disk (Markwardt, Swank, & Taam 1999; Trudolyubov et al. 1999; Muno, Morgan & Remilland 1999; Sobczak et al. 2000). It is possible that the QPOs trace the Keplerian motion at the inner radius of the observable disk (Belloni et al. 2000). We note that the other two micro-quasars XTE J1550-564 (Wijnands et al. 1999; Cui et al. 2000) and GRO J1655-40 (Remillard et al. 1999; Cui et al. 1999) have different types of QPOs too. Study of the QPO properties in GRS 1915+105 can provide important information of the accretion flow in this source as well as other micro-quasars.

Complex phase/time lags have also been observed for the QPOs of GRS 1915+105. Cui (1999) found that the hard lags of the low-frequency QPOs in GRS 1915+105 alternate from negative to positive values as the frequency increases from the fundamental to higher harmonic frequencies, and the high frequency QPOs always show hard phase lag. The intermediate frequency QPOs were studied by Lin et al. (2000) and Reig et al. (2000). They found that the hard lags of these QPOs, different from the phase lags of the low-frequency QPOs, alternate from positive to negative values as the frequency increases from 0.5 to 10 Hz. The similar timing characteristics were also observed in XTE J1550-564 (Cui, Zhang & Chen 2000). According to the phase lags of GRS 1915+105, the intermediate frequency QPOs can be further classified into three types: (1) the 0.5-2 Hz QPOs, whose hard lags at the fundamental and first harmonic frequencies are both positive; (2) the 2-4.5 Hz QPOs, whose hard lags are negative at the fundamental frequency but positive at the first harmonic frequency; (3) the 4.5-10 Hz QPOs, which show negative phase lags at both the fundamental and harmonics (Lin et al 2000a; Reig et al. 2000).

It is suggested that the 0.5-10 Hz QPOs observed during state C provide a link between the optically thick accretion disk and the Comptonization region (Muno et al.

2001). Since the accretion disk has temperature structures and the Comptonization region could up-scatter the lower energy photons into higher energy ones, the energy dependence of different types of QPOs and their phase lags can set strong constraints on the current accretion disk models and provide another avenue to explore the origin of phase lags of GRS 1915+105. According to the drifting blob model, the centroid frequency of a QPO is a function of the photon energy. The energy-dependence of the fractional rms and phase lags of the QPOs have been widely studied (Morgan et al. 1997; Cui 2000; Cui et al. 1999; Lin et al. 2000a; Reig et al. 2000; Rodriguez et al. 2004). For $\sim$ 4 Hz QPO of XTE J1550-564, Sriram et al.(2007) found a frequency difference at two energy bands(2-20keV and 20-50keV). Choudhry et al. (2005) found that the centroid frequency of the 3$\sim$4 Hz QPOs at 2-7 keV is higher than those in 20-50keV in GRS J1915+105. However, as a parameter of the theoretical model of the QPOs, the relations between the QPO centroid frequency and photon energy in GRS 1915+105 and other microquasars have not been well studied yet.

Since photons with different energies are usually from regions with different physical properties, the energy-dependence of QPOs can provide additional information that may be critical for a better understanding of the QPO origins. Therefore, we present in this paper a study of the energy dependence of the centroid frequencies of the 0.5-10 Hz QPOs. In section 2, we describe the data and how they were analyzed. The main results are given in section 3, their physical implications are discussed in section 4, and section 5 is a short summary of this work.

2. Data Reduction and Analyses

To evaluate the energy-dependence of the QPO centroid frequency, we select the *RXTE* observations published in Morgan et al. (1997), which show the 0.5-10 Hz QPOs

and have enough exposure time for each observation to evaluate the QPOs. In these observations (Table 1), GRS 1915+105 was in class χ of state C in the classification by Belloni et al. (2000) or in the plateau state (Fender 2001), because these observations didn't show strong variability, HR_2(13-60 keV/2-5 keV)$>$ 0.1, and the original disk contribution is expected to be very soft here. The timing and spectral properties of GRS 1915+105 in those observations have been widely studied previously. For example, Lin et al. (2000a) and Reig et al. (2000) have investigated the phase-frequency dependence of the QPOs, while Muno et al. (2001) and Trudolyubov et al. (1999) have reported its energy spectral properties. The QPO centroid frequency is relatively stable over each *RXTE* epoch in these observations. Therefore they are very suitable to study the energy dependence of the centroid frequencies of the QPOs.

Table 1

The data are reduced by using the FTOOLS package as described by Qu, Yu & Li (2001). The timing analyses include calculations of the power density spectrum (PDS) and the cross-power spectrum (CPS), using the binned mode and event mode data respectively. According to the data modes of the observations, we extract the light-curves of GRS 1915+105 with a time resolution of $\sim$ 4 ms (2^{-8} s) in seven PCA energy bands defined in Table 2. Among these energy bands, the hardest energy band (Channels 50-103) has the lowest statistics, and its mean count rate is still about 320 cts/s with the model predicted background count rate of 16 cts/s. In every energy channel, the quality factor ($Q = f/\Delta f_{FWHM}$) of the 6 Hz QPO that presented in the observation is greater than 4, permitting a detailed study on the relations between the QPO frequency, photon energy, and phase lag.

Table 2

The PDS is fitted with a model including a power law to represent the continuum

plus one or two Lorentzians to represent the QPOs. However, it is difficult to obtain a statistically acceptable fit to the PDS exactly between 1/16 and 16 Hz. For an example, we fit the 1/16 to 16 Hz PDS of observation (10408-01-32-00) that shows a 6 Hz QPO with a power law plus three Lorentzians, the reduced χ^2 is 6.5. If we limit the frequency range as 4 to 8 Hz, the fit is improved apparently, with $\chi^2 < 1.6$. Thus in order to get the accurate centroid frequency and the full width at half maximum (FWHM) of the QPO in 2-13 keV, the frequency range is selected to cover the QPO and to make the reduced χ^2 close to the minimum (see Table 1), similar to that used by Cui (1999). The PDSs in the other energy bands are fitted in the same frequency range by the model forenamed. The errors of the model parameters are derived by varying the parameters until $\Delta\chi^2 = 1$.

The phase lags ϕ of the QPOs are calculated by averaging the phase lags over the frequency range from $f_{\rm QPO}$-FWHM/2 to $f_{\rm QPO}$+FWHM/2. Their errors are estimated from the standard deviation of the real and imaginary parts of the CPSs (Cui et al. 1997). Figure 1 shows two example PDSs in energy bands of 2-5 keV and 18-38 keV as well as the CPSs between these two energy bands. Apparently, the centroid frequency of the QPO around $\sim$ 6 Hz has a higher value in the harder energy band. The inset in this figure also shows that the fitting method above-mentioned gives reasonable fits to the PDSs.

Figure 1

3. Results

We find that the centroid frequencies of QPOs are related with photon energy. This relation evolves from a negative correlation to a positive one when the QPO frequency increases. Figure 2a shows such relations for a few typical QPOs. The energy-dependence of the centroid frequency of the QPO can be fitted by a power-law, and the fitted results

are listed in Table 3. For QPOs with the centroid frequencies lower than 3 Hz, the centroid frequency decreases monotonically with photon energy, but the correlation becomes weaker with the centroid frequency increases. For QPOs with the centroid frequencies higher than 3 Hz, the centroid frequency increases significantly with photon energy, and the correlation also becomes stronger as shown by the correlation coefficients. However, for QPOs around 3 Hz, their centroid frequencies don't have a monotonic evolutionary trend with photon energy, while the values of the correlation coefficients turn over their sign from negative to positive.

table 3

The relation between phase lag and photon energy is opposite to that between QPO centroid frequency and photon energy. The results of fitting and correlation coefficient are listed also in Table 3 and displayed in Figure 2b. When the QPO frequency is around 1 Hz, the phase lag is positively correlated with photon energy, and the two quantities become negatively correlated when the QPO frequency reaches above 3.5 Hz. These results are similar to the ones of Lin et al. (2000a) and Reig et al. (2000).

Figure 2

In Figure 3 we plot the centroid frequency variation Δf and phase lag ϕ versus the QPO frequency for all the QPOs we detected in the observations. Both Δf and phase lag are calculated between two energy bands of 2-5 keV and 13-18 keV only. It is shown that Δf increases with the QPO frequency, while the phase lag decreases, indicating a negative correlation between Δf and ϕ for the QPOs.

Figure 3

The negative correlation between Δf and ϕ holds not only among different QPOs but also within a QPO. The Δf and ϕ calculated between 2-5 keV and the other five higher

energy channels (Table 2) for a few typical QPOs are shown in Figure 4. The results show that Δf and ϕ has an anti-correlation for QPOs with centroid frequency lower than 2 Hz or higher than 3.5 Hz, and no correlation for QPOs between 2 and 3.5 Hz. We calculate the correlation coefficients and fit the relation with a linear function to all the QPOs we detected in this work. The results are listed in Table 4.

Table 4

4. Discussions

For the first time we find the centroid frequency evolution with photon energy for the 0.5-10 Hz QPOs of GRS 1915+105. We also find that the QPO phase lag is correlated with both photon energy and QPO frequency. The QPO centroid frequencies are shown to have an anti-correlation with the phase lags, as shown in Figure 4. These results set strong constraints on the current models of the origin of QPOs and phase lags in black hole binaries, and make a direct challenge for theorists to explain the new observable phenomena.

Various models have been proposed to explain the timing phenomena in black hole binaries. It is generally believed that the X-ray radiation of a black hole binary is contributed by three components: the soft X-ray radiation from the accretion disk, the hard components from the Compton cloud and/or jet (McClintock & Remillard 2003). The QPOs are suggested to be related to the accretion disk of the compact object, while the phase lags to the electron cloud. Particularly, the 0.5-10 Hz QPOs of GRS 1915+105 could occur in the inner region of the disk and are associated with disk instabilities (see van der Klis 2004 and McClintock & Remillard 2003 for review). However, GRS 1915+105 displays the number of X-ray states, many models for microquasar behavior are based on a limited

number of its X-ray states. Based on our observational results, we only discuss the following four models commonly used to to describe the origin of QPOs in compact objects: (1) The global disk oscillation (GDO) model; (2)The radial and orbital oscillation model (ROOM); (3) The accretion flow instability model (AFIM); and (4) the drift blob model (DBM).

4.1. Constraints from the energy dependent QPO frequency

For orbital and epicyclic frequency models, the particles moving around the compact objects could have different oscillating frequencies in the inner region of the accretion disk: orbital, radial and vertical epicyclic frequencies. Damping, or the superposition of many local frequencies can turn the intrinsically periodic disk oscillations into QPOs or broad noise. In the global disk oscillation (GDO) model, the disk oscillation is a vertical mode, and the GDO frequency is expected to be also independent of the photon energy and should be seen in all the energy bands that disk emits (Titarchuk 2000). Thus the GDO model can not explain the observational phenomena of the intermediate-frequency QPOs.

For the radial and orbital oscillation model (ROOM), the oscillation frequency is a function of the disk radius/temperature (Nowak & Wagoner 1993; Nowak 1994). The QPO frequency will vary with energy because photons with different energies are from different radii. These models can therefore explain qualitatively the evolution of the QPO frequency with energy. However, the emission from the disk is thermal. There should be a break of the QPO power represented by the root-mean-square (RMS) at higher energy if the oscillations occur in the inner region of the disk, since the high energy emission is from the Compton cloud (Rodriguez et al. 2004). However, such a break has not been detected up to ~ 30 keV, making the disk oscillation model of the QPOs unlikely. Meanwhile, the ROOM can not explain the various correlations between the centroid frequency and photon energy for different QPOs. The ROOM model need to be greatly modified in order to fit

the observational results.

In the accretion flow instability model (AFIM), locally at each radius the disk fluctuates on different instability timescales, and the oscillations propagate in the disk (Nowak 1994). In this scenario, emission from the inner region of the disk tends to have a higher QPO frequency and a harder spectrum. This model can naturally explain the observed positive correlation between the centroid frequency and photon energy for the QPOs with frequency higher than ∼3.5 Hz. But the observed negative correlation for QPOs less than 2 Hz contradicts the model prediction.

The energy-dependence of the QPO frequency is expected by the drift blob model (DBM; Böttcher & Liang 1998, 1999; Hua et al. 1997). In this model, the Keplerian motion of the blobs could manifest itself in a QPO observationally, and any radial drift of the blobs would cause the QPO frequency to increase with energy. Similar to the AFIM model, the DBM model can explain the observed properties of the QPOs higher than ∼3 Hz, but not for the QPOs less than 2 Hz. The relation between model and observed phenomena is summarized in table 5.

Of the models we considered above, none can fully explain the energy dependencies of QPOs obtained in this paper. The energy dependencies of the QPO centroid frequencies provide additional information for theoretical models. And the new observable properties of the QPOs of the GRS 1915+105 also make a challenge to the new models of the QPOs, i.e, the new theoretical model should not only reproduce or explain the observable phenomena in this paper, but also explain the other properties such as the energy dependence of the rms and the phase lags (Cui 1999, Rodriguez et al. 2004).

Here insert Table 5

4.2. Phase lag results and their constraints on models

To explain the observational phase (time) lags in the compact X-ray objects, a lot of models are proposed (see Cui 1999; Poutanen 2001 for review, and reference therein). Among them, the so called standard model and the perturbation propagation model are the two major ones. In the standard model, the time lag is considered as the diffusion timescale of the photon passing through the Comptonization region (Cui 1999; Poutanen 2001). The hard lag is the result of the process in which the soft (seed) photons gain energy from the hotter electron corona. For the perturbation propagation model, the soft phase lags can be explained by assuming that perturbations propagate from the inner disk to the outer disk. There may also be perturbations propagating inward from the outer edge of the disk, which generate hard phase lags (Lin et al. 2000b).

The observed phase lag behaviors in this paper challenge the above two models. Since the standard model only predicts hard lags, the measured soft lags in GRS 1915+105 are incompatible with the model (see also Cui 1999), and furthermore, the observed large time lag values require a huge corona size ($\sim 3 \times 10^{10}$cm) that is physically unrealistic (Hua, Kazanas & Cui 1999). Although the perturbation propagation model can explain the observed soft and hard lags qualitatively, it is not clear how the propagation direction of the perturbation transits when QPO frequency passes 2 Hz, at which the phase lag of the QPO changes sign as revealed in this work. Probably the phase lags are of multiple origins.

The anti-correlations between the phase lags ϕ and frequency variation (Δf) of the QPOs (see also Figure 4), and between Δf and $\log(E)$, imply that the phase lags could be caused by the change of the QPO frequency, which may give a new approach to explain the phase lags in the compact X-ray objects. To better illustrate this point, we derived the relation between the phase lag and Δf as follows.

According to the definition of the cross correlation function, $ccf(\tau) = \int_{-\infty}^{\infty} h(t)s(t-\tau)dt$,

the cross power spectrum is $CPS(\nu) = \int_{-\infty}^{\infty} ccf(\tau) e^{i2\pi f \nu \tau} d\tau = S^*(\nu) H(\nu)$, i.e.,

$$\begin{aligned} CPS(\nu) &= |S^*| e^{-i\phi_s(\nu)} |H| e^{i\phi_h(\nu)} \\ &= |S^* H| e^{i(\phi_h(\nu) - \phi_s(\nu))} \\ &= A e^{i\phi(\nu)} \end{aligned}$$

where, $S^*(\nu) = |S^*| e^{-i\phi_s(\nu)}$ and $H(\nu) = |H| e^{i\phi_h(\nu)}$. If the light curves with oscillations in two different energy bands could be described by $s(t) = s(ft)$ and $h(t) = h((f + \Delta f)t)$, then,

$$\begin{aligned} CPS(\nu) &= \frac{1}{f(f + \Delta f)} S^*(\frac{\nu}{f}) H(\frac{\nu}{f + \Delta f}) \\ &= A e^{i[\phi_h(\frac{\nu}{f+\Delta f}) - \phi_s(\frac{\nu}{f})]} \end{aligned}$$

So the phase lag is,

$$\begin{aligned} \phi(\nu) &= \phi_h(\frac{\nu}{f + \Delta f}) - \phi_s(\frac{\nu}{f}) \\ &\approx \phi_h(\frac{\nu}{f}(1 - \frac{\Delta f}{f})) - \phi_s(\frac{\nu}{f}) \\ &\approx \phi_h(\frac{\nu}{f}) + \phi_h'|_{\frac{\nu}{f}} \times \frac{\nu \Delta f}{f^2} - \phi_s(\frac{\nu}{f}) \end{aligned}$$

If let $\nu = f$, the phase lag of the QPO with frequency f is,

$$\begin{aligned} \phi(f) &= \phi_h(f) - \phi_s(f) + \phi_h'(f) \times \frac{\Delta f}{f} \\ &= \phi_\lambda(f) + \phi_f(\Delta f) \end{aligned}$$

where, $\phi_\lambda(f) = \phi_h(f) - \phi_s(f)$ is phase lag due to physical processes such as Comptonization and $\phi_f(\Delta f) = \phi_h'(f) \times \frac{\Delta f}{f}$ is caused by the change of the oscillation frequency of the QPO. $\phi_f(\Delta f) = k_{model} \Delta f = k_f \frac{\phi_h'}{2\pi} \Delta f$ ($k_{model} \propto k_f = \frac{2\pi}{f}$), i.e., the phase lag caused by the change of the QPO frequency is proportional to $-\Delta f$.

If the observed phase lag is due to the change of the QPO frequency, the k_{obs} should be proportional to k_f, where k_{obs} is the fitted slop between ϕ and Δf. In Table 4 we list k_f and k_{obs} as well as the correlation coefficient between them. However, there is not an obvious correlation between k_{obs} and k_f, which means that the measured phase lags are caused partially by the change of the QPO frequency. These results, together with k_{obs} and k_f, show that the phase lag caused by Δf is a small fraction of the observed phase lags for QPOs less than 2 Hz but becomes dominant for QPOs with $f \geq$3.5 Hz.

5. Summary

We find that the frequency and phase-lag are both energy dependent for the 0.5-10 Hz QPOs in GRS 1915+105. For QPOs with the centroid frequencies less than 3 Hz, the centroid frequency decreases monotonically with photon energy. For QPOs with the centroid frequencies larger than 3 Hz, the centroid frequency increases significantly with photon energy. However, for the QPOs around 3 Hz, the centroid frequencies of the QPOs don't have a monotonic evolutionary trend with photon energy (see Figure 2 and Table 3). Meanwhile, the phase lag behaviors are closely related to the variables of the QPO centroid frequency. The phase lag is negatively correlated with the centroid frequency difference of the QPO when QPO frequency larger than 3.5 Hz or less than 2 Hz. No correlation for phase lag and centroid frequency of the QPOs is found between 2 and 3.5 Hz. Of the models we considered, none can fully explain all the properties of QPOs obtained in this paper (see Table 5).

It is shown that the observed phase lag may be caused by two mechanisms, one is the comptonization of the soft photon, another is caused by the frequency difference of the QPO at different energy bands. The frequency difference between two energy bands could be a main source of the phase-lag for QPOs with $f \geq$ 3.5Hz. However, it is necessary to

further investigate the energy dependence of the QPOs in micro-quasars for verification generally. Meanwhile, many of the models proposed are actually variability-frequency models, which predict the frequency, or the power spectrum, of the fluctuations only in physical flow parameters rather than in any observable quantity. In order to allow further tests of QPO models and to discriminate between them, predictions of the observable of the oscillations are essential. However, the new phenomena in this paper make a direct challenge to the theoretical model for the QPO. A successful model should be able to reproduce the energy-dependencies of the QPO centroid frequencies we observed, but also the correlations between Δf and phase lags should be explained.

The authors would like to thank anonymous referee for some helpful suggestions and comments. This work was partially supported by the National Basic Research Program of China (Grant No. 2009CB824800), the Natural Science Foundation of China (Grant No. 10773017), the Natural Science Foundation of Xinjiang Uygur Autonomous Region of China (Grant No. 200821164), and the Program of the Light in Chinese Western Region (LCWR)(Grant No. LHXZ 200802)

REFERENCES

Belloni, T., Méndez, M., King, A.R., van der Klis, M., & van Paradijs, J. 1997a, ApJ 479, L145

Belloni, T., Méndez, M., King, A.R., van der Klis, M., & van Paradijs, J. 1997b, ApJ 488, L109

Belloni, T., Klein-Wolt, M., Méndez, M., van der Klis, M., & van Paradijs, J. 2000, A&A, 355, 271

Böttcher, M., & Liang, E. P. 1998, ApJ, 506, 281

Böttcher, M., & Liang, E. P. 1999, ApJ, 511, L37

Chakarabarti, S.K., and Manickram, S.G. 2000, ApJ, 531, L41

Choudhury, M., Rao, A. R., Dasgupta, S., Pendharkar, J., et al. 2005, ApJ, 631, 1072

Cui, W., Zhang, S. N., Fock, W., and Swank, J. H. 1997, ApJ, 484, 383

Cui, W., Zhang, S. N., Chen, W. 1998, ApJ, 492, L53

Cui, W. 1999, ApJ, 524, L59

Cui, W., Zhang, S.N., Chen, W., & Morgan, E.H. 1999, ApJ, 512, L43

Cui, W., Zhang, S.N., & Chen, W. 2000, ApJ, 531, L45

Fender, R.P. 2001, MNRAS, 322, 31

Fender, R.P. 2005, in Compact Stellar X-Ray Sources, ed. W. H. G. Lewin & M. van der Klis (Cambrige: Cambrige Univ. Press), in press(astro-ph/0303339)

Hua, X.-M., Kazanas, D., & Titarchuk, L. 1997, ApJ, 482, L57

Hua, X.-M., Kazanas, D., & Cui, W. 1999, ApJ, 512, 793

Ji, J.F., Zhang, S.N., Qu, J.L., Li, T.P. 2003, ApJ, 584, L23

Lin, D., Smith, I. A., Liang, E. P., & Böttcher, M.B. 2000a, ApJ, 543, L141

Lin, D., Smith, I. A., Böttcher, M., & Liang, E. P. 2000b, ApJ, 531, 963

McClintock, J.E., & Remillard R.A. 2003, in "Compact Stellar X-ray Sources," eds. W.H.G. Lewin & M. van der Klis, (Cambridge: Cambridge U. Press), astro-ph/0306213

Miller, J. M., & Homan, J., 2005, ApJ, 618, L107

Morgan, E. H., Remillard, R. A., & Greiner, J. 1997, ApJ, 482, 993

Muno, M.P., Remillard, R.A., Morgan, E.H., et al. 2001, ApJ, 556, 515

Nowak, M. A. 1994, ApJ, 422, 688

Nowak, M. A., & Wagoner R.V. 1993, ApJ, 418, 187

Poutanen, J. 2001, in X-ray astronomy: "Stellar Endpoints, AGN, and the Diffuse X-ray Background," Ed. N.E. White, G. Malaguti, and G.G.C.P. Melville, 599, 310.

Qu, J.L., Yu W. & Li T.P. 2001, ApJ, 555, 7

Reig, P., Belloni, T., van der Klis, M., et al. 2000, ApJ, 541, 883

Rodriguez, J., Corbel, S., D. C. Hannikainen, D.C., et al. 2004, ApJ, 615, 416

Sobczak, G.J., McClintock J. E., Remillard, R.A., et al. 2000, ApJ, 531, 537

Sriram, K., Agrawal, V. K., Pendharkar, J. K., Rao, A. R., 2007, ApJ, 661, 1055

Titarchuk, L. 2000, ApJ, 542, L111

van der Klis, M. 2004, in Compact stellar X-ray sources, Ed. Lewin & van der Klis (eds), Cambridge University Press (astro-ph/0410551).

This manuscript was prepared with the AAS LaTeX macros v5.2.

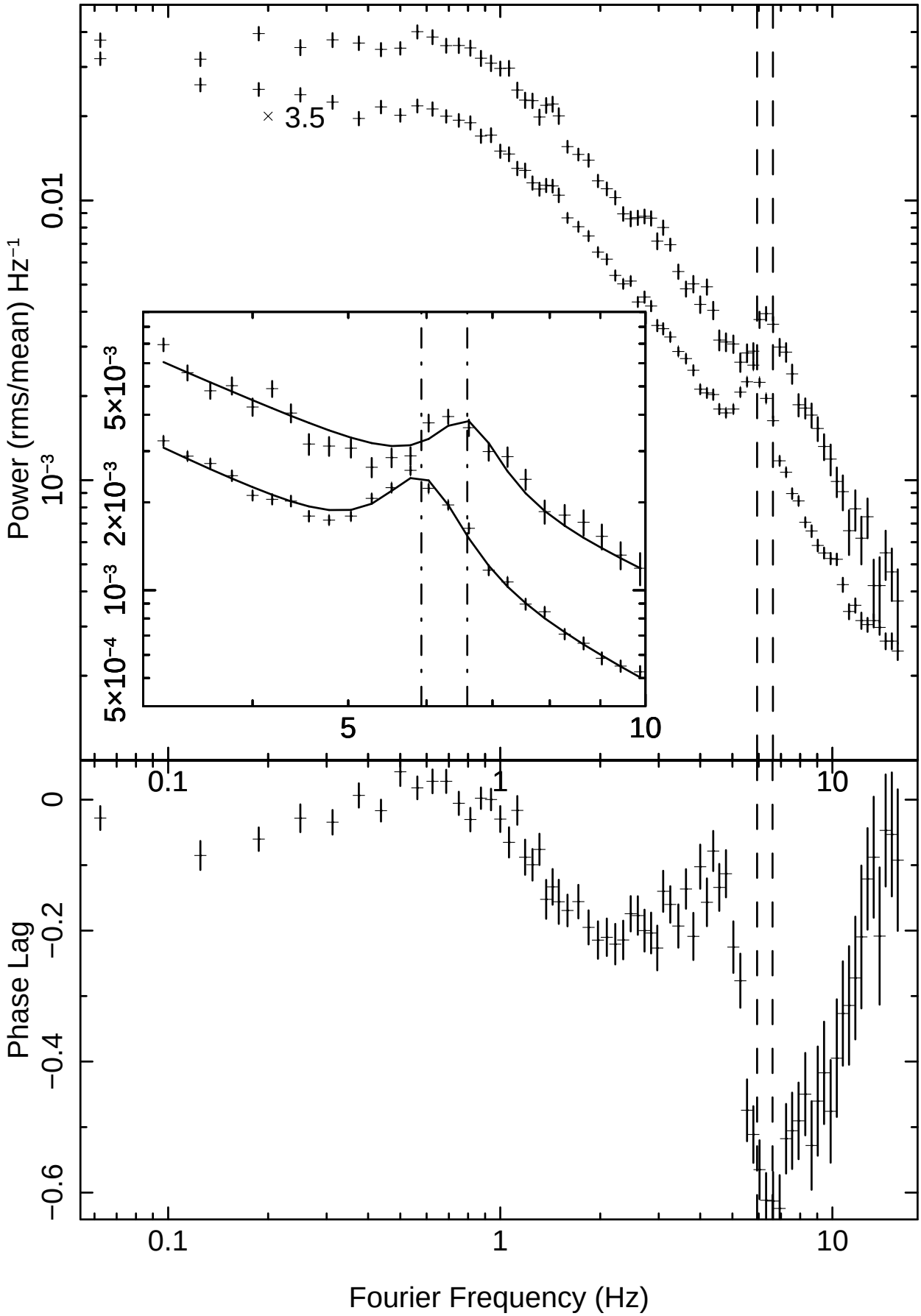
× 3.5
Power (rms/mean) Hz⁻¹
0.01
10⁻³
5×10⁻³
2×10⁻³
10⁻³
5×10⁻⁴
5
10
0.1
1
10
Phase Lag
0
−0.2
−0.4
−0.6
0.1
1
10
Fourier Frequency (Hz)

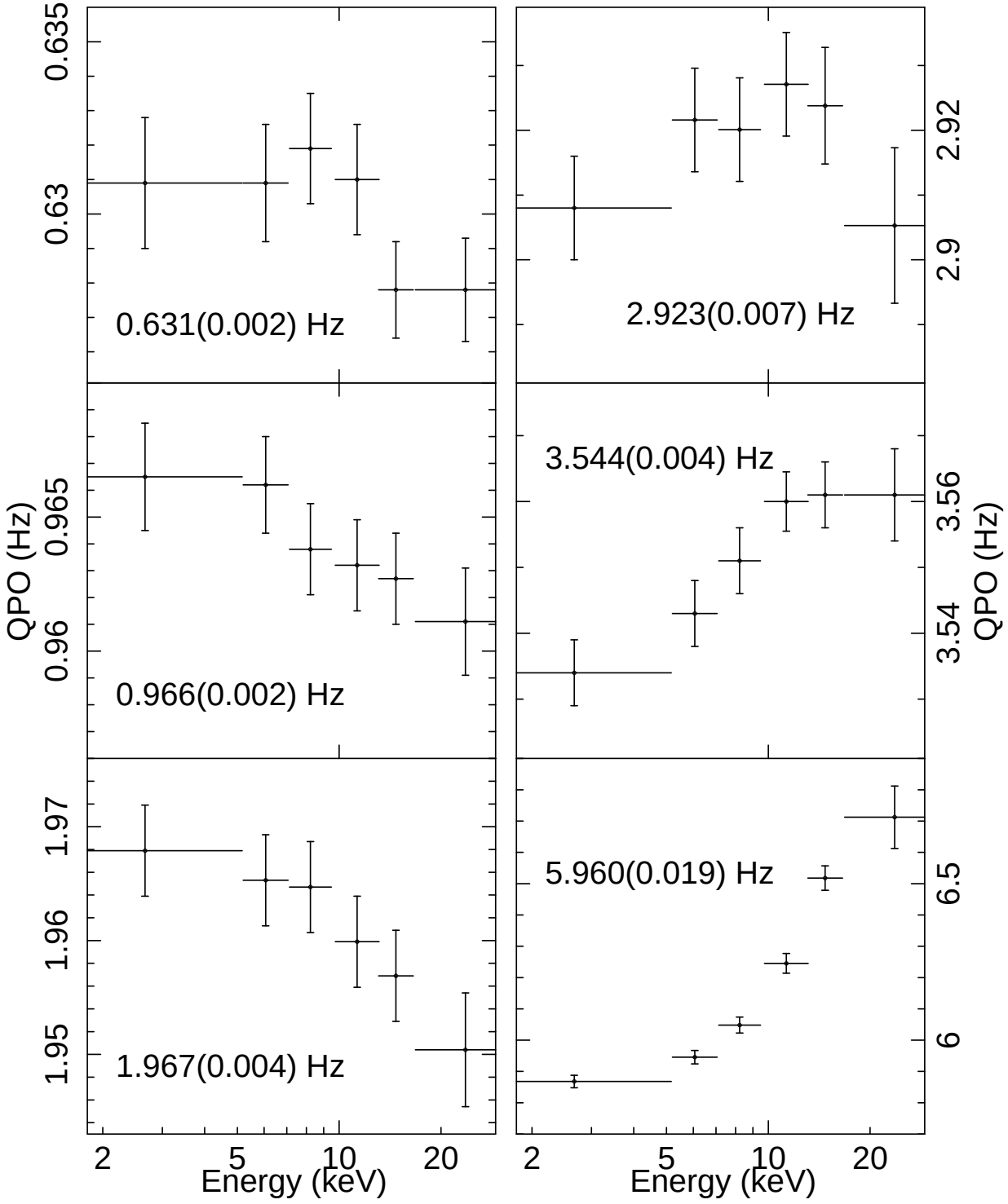

Fig. 2.— a): The relation between the QPO centroid frequency and photon energy for a few typical QPOs. The digit in each panel is the centroid frequency of the QPO at 2-13 keV.

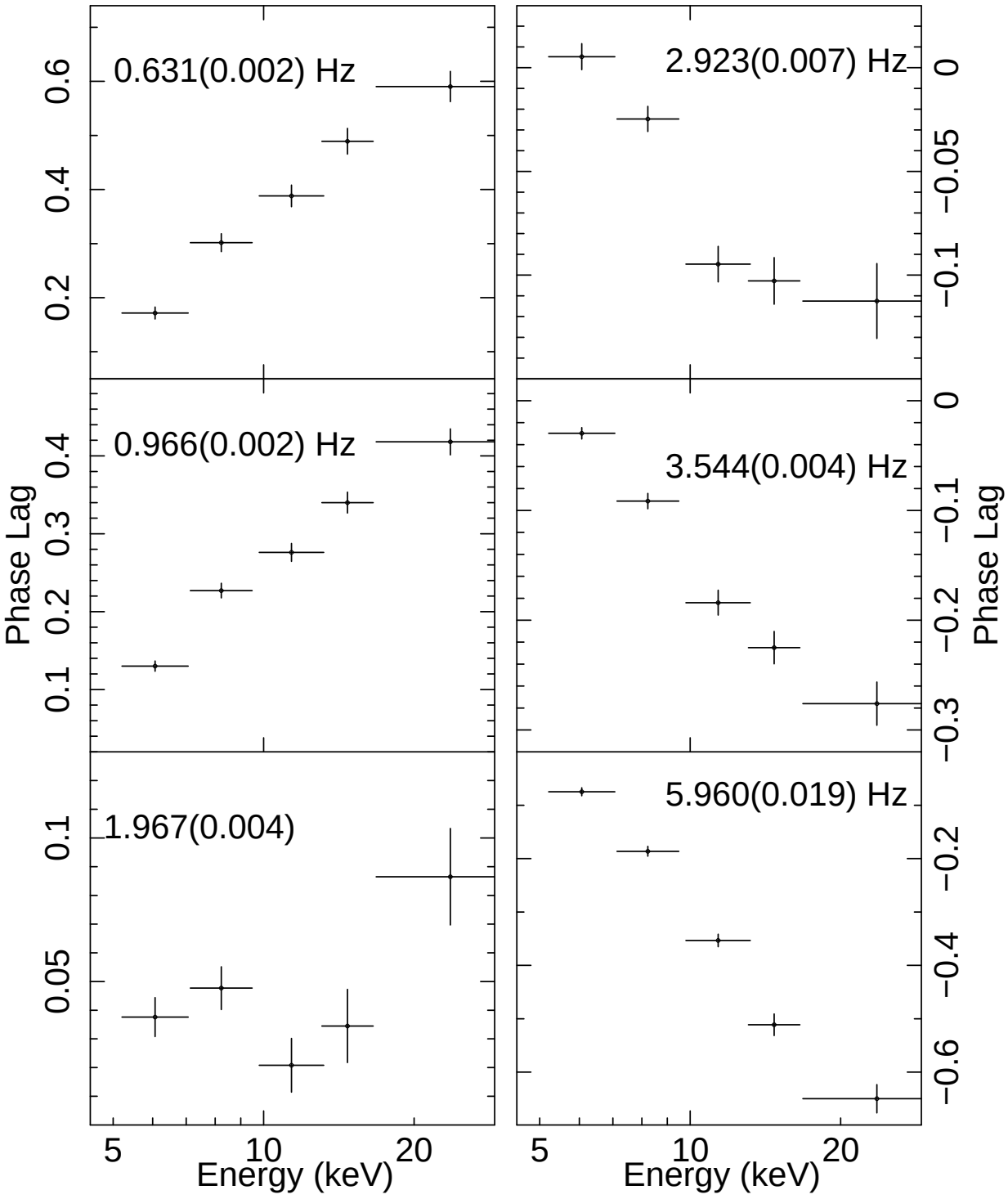

Fig. 2.— b): The relation between phase lag and photon energy for a few typical QPOs.

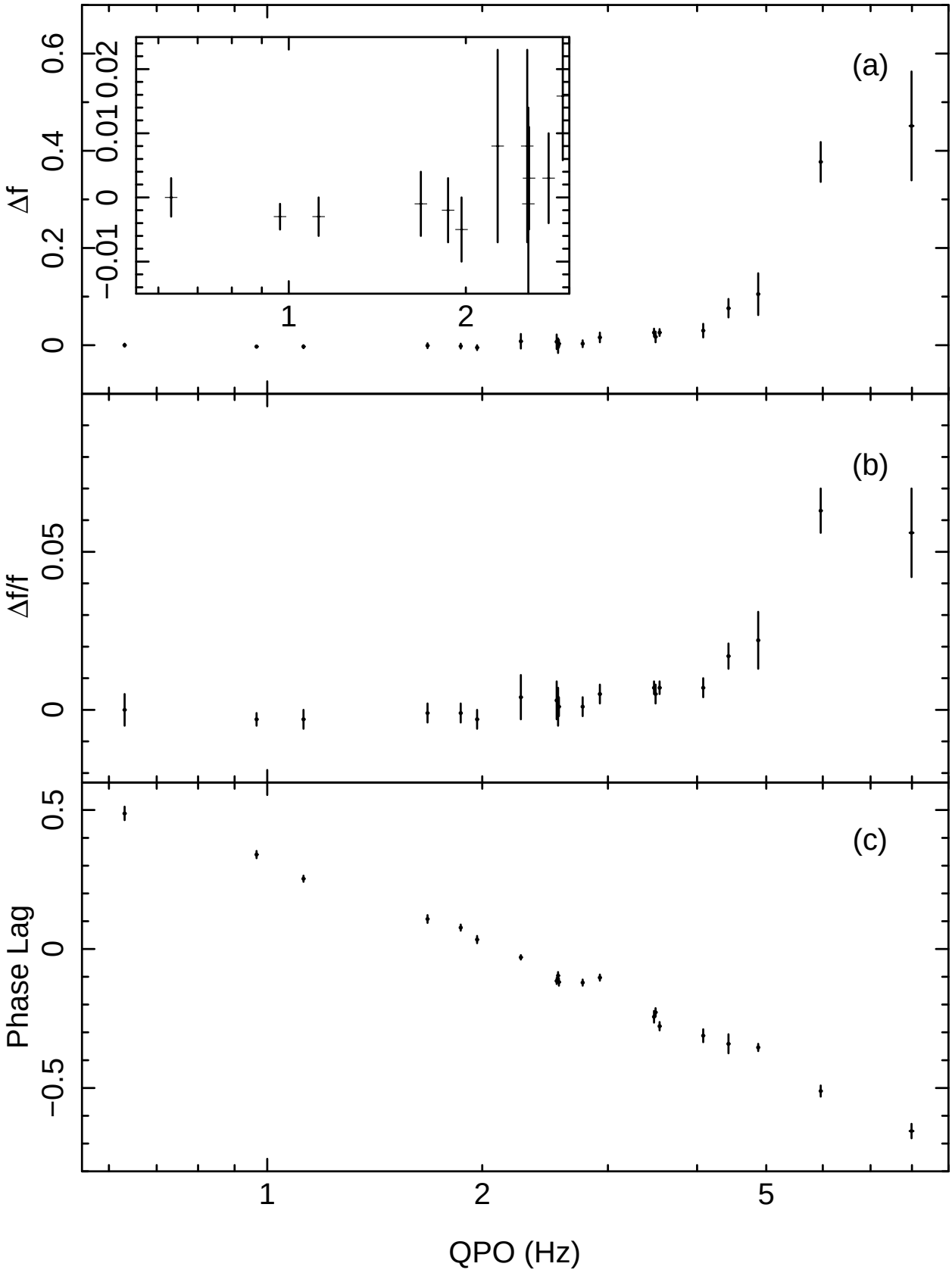

Fig. 3.— QPO frequency differences and phase lag vs QPO frequency for energy bands 2-5 keV and 13-18 keV. The inset show the Δf of the QPOs with frequencies less than 3 Hz.

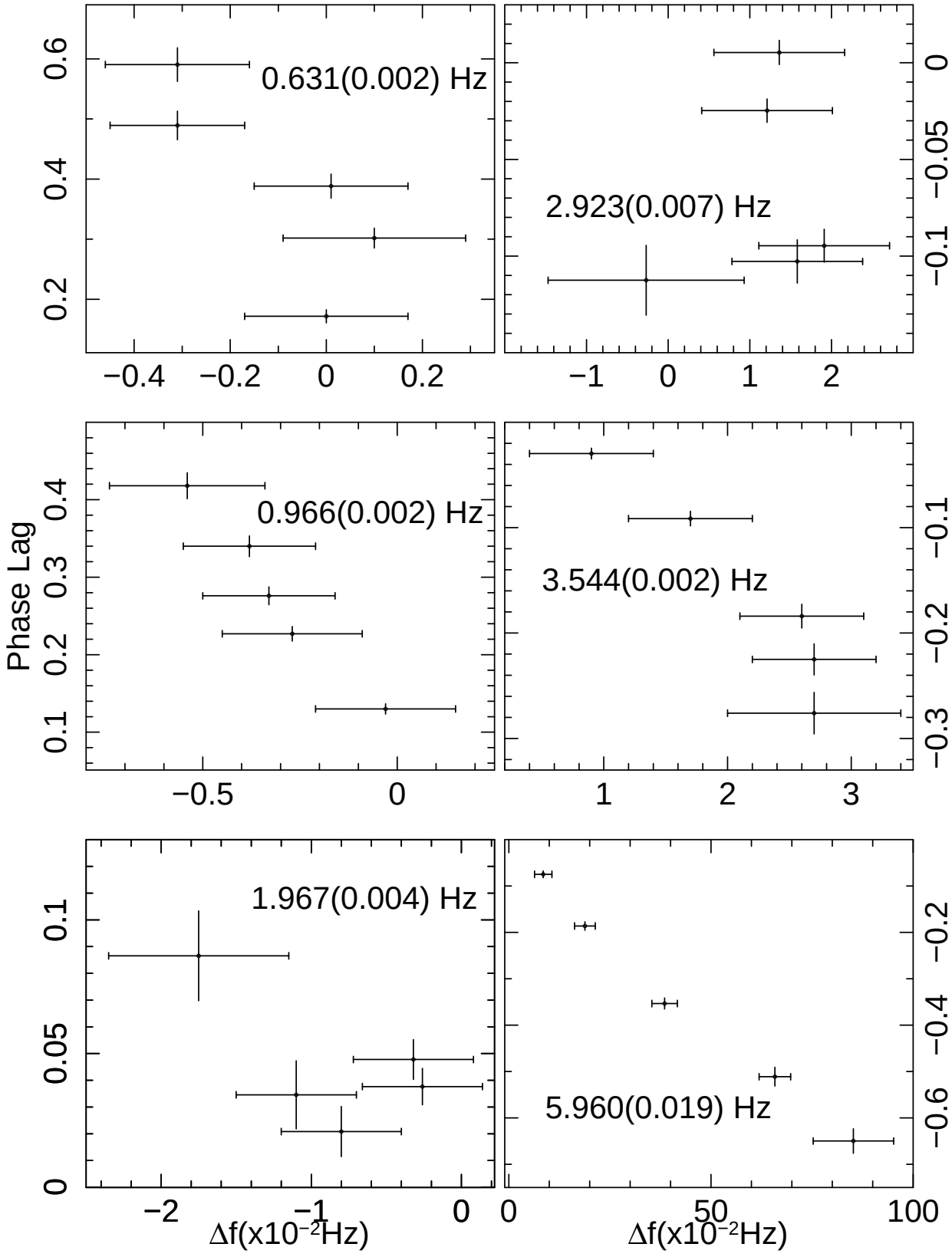

Fig. 4.— Frequency differences(Δf) vs phase lags (ϕ) for various typical QPOs. The digits are the centroid frequencies of the QPOs at 2-13 keV. Refer to the text for detail.

Table 1. The RXTE Observations of GRS 1915+105 used in this paper

ObsID	Date	Exposure(s)	f_c/(Fitting range)
21-02	07/07/96	2000	7.988 ± 0.051/(4.5-12)
22-00	11/07/96	2520	3.479 ± 0.005/(1.8-6.5)
22-01	11/07/96	3320	2.770 ± 0.005/(1.7-9)
22-02	11/07/96	3312	2.554 ± 0.006/(0.16-4.2)
23-00ab	14/07/96	6640	3.544 ± 0.005/(2-10)
24-00ab	16/07/96	6544	2.266 ± 0.006/(1.6-6.5)
24-00cd	16/07/96	6544	2.543 ± 0.005/(1.6-6.5)
25-00	19/07/96	3328	1.125 ± 0.002/(0.2-1.8)
27-00	26/07/96	8960	0.631 ± 0.002/(0.4-2)
28-00	03/08/96	9984	0.966 ± 0.002/(0.2-2.9)
29-00a	10/08/96	2952	1.677 ± 0.004/(0.8-4.6)
29-00b	10/08/96	3392	1.866 ± 0.004/(0.8-4.6)
29-00c	10/08/96	3392	1.967 ± 0.004/(0.8-4.6)
30-00	99/08/98	9960	4.871 ± 0.011/(1.8-10)
31-00a	25/08/96	2208	4.092 ± 0.007/(2.6-6)
31-00b	25/08/96	2912	4.434 ± 0.011/(2.5-8.8)
31-00c	25/08/96	2912	3.505 ± 0.008/(2.2-7.4)
32-00	31/08/96	7424	5.960 ± 0.019/(3-10)
*49-00	08/10/97	3408	2.923 ± 0.007/(1.4-15)

21-02=10408-01-21-02; ab=a+b; *49-00=20402-01-49-00;

f_c is the QPO frequency at PCA channel 2-13 keV

separate

Table 2. RXTE/PCA Energy to Channel Table

PCA Channel	Energy Range(keV)	Centroid Energy (keV)
0-35	1.94-12.99	6.39
0-13	1.94-5.12	2.67
14-18	5.12-6.89	6.06
19-25	6.89-9.39	8.22
26-35	9.39-12.99	11.30
36-49	12.99-18.09	14.72
50-103	18.09-38.44	23.63

Table 3. Energy-dependence of the QPO frequencies and phase lags

		E$-f_{\rm QPO}$			E$-\phi$			
ObsID	f_c	$\Gamma(\times10^{-3})$	χ^2	Cor	ϕ^+	Γ	χ^2	Cor
21-02	7.988 ± 0.051	45.0 ± 6.7	6.1	0.98	-0.655 ± 0.026	1.17 ± 0.33	1.75	-0.97
32-00	5.960 ± 0.019	49.0 ± 3.1	76.5	0.97	-0.511 ± 0.020	0.97 ± 0.13	5.98	-0.96
31-00a	4.092 ± 0.007	3.1 ± 1.3	3.2	0.78	-0.312 ± 0.023	0.69 ± 0.39	1.01	-0.92
23-00	3.544 ± 0.005	4.3 ± 0.9	2.1	0.81	-0.278 ± 0.015	0.78 ± 0.42	0.75	-0.95
22-00	3.479 ± 0.005	3.9 ± 1.0	2.7	0.83	-0.244 ± 0.021	0.80 ± 0.50	0.35	-0.75
49-00	2.923 ± 0.007	-1.2 ± 1.8	3.8	-0.29	-0.103 ± 0.011	0.45 ± 0.35	0.06	-0.87
22-01	2.770 ± 0.005	-1.1 ± 1.4	6.4	-0.71	-0.121 ± 0.011	0.61 ± 1.6	0.08	-0.91
22-02	2.554 ± 0.006	-6.6 ± 1.4	3.4	-0.69	-0.096 ± 0.013	0.63 ± 5.0	0.02	-0.92
29-00c	1.967 ± 0.004	-3.2 ± 1.4	1.1	-0.99	0.034 ± 0.013	$0.62^{+0}_{-\infty}$	0.01	0.57
25-00	1.125 ± 0.002	-4.2 ± 1.3	1.94	-0.997	0.253 ± 0.011	0.65 ± 0.26	0.453	0.93
28-00	0.966 ± 0.002	-3.2 ± 0.2	0.48	-0.94	0.340 ± 0.013	0.66 ± 0.15	1.35	0.94
27-00	0.631 ± 0.002	0.52 ± 1.5	2.58	-0.80	0.489 ± 0.024	0.067 ± 0.027	2.0	0.94

Cor=Correlation coefficient; Γ is power index of the relation between Δf or ϕ and photon energy E.

The phase lag ϕ^+ is obtained between 13-18 keV and 2-5 keV energy bands;

Reduced χ^2=$\chi^2/(6-2)$

Table 4. The relation between frequency differences (Δf) and phase lags (ϕ) of the QPOs

ObsID	f_c	k_{obs}	χ^2	Cor	k_f
21-02	7.988 ± 0.051	-1.08 ± 0.30	1.47	-0.99	-0.79
32-00	5.960 ± 0.019	-0.694 ± 0.093	0.677	-0.99	-1.1
31-00a	4.092 ± 0.007	-1.1 ± 7.4	4.15	-0.90	-1.5
23-00	3.544 ± 0.005	-12.9 ± 6.8	0.7	-0.94	-1.8
22-00	3.479 ± 0.005	-8.0 ± 8.0	2.0	-0.59	-1.8
49-00	2.923 ± 0.007	0.5 ± 8.4	0.10	-0.08	2.1
22-01	2.770 ± 0.005	2.3 ± 6.4	0.15	0.48	2.3
22-02	2.554 ± 0.006	3.5 ± 17	0.03	0.64	2.5
29-00c	1.967 ± 0.004	-3.3 ± 18	0.01	-0.78	-3.2
25-00	1.125 ± 0.002	-20.3 ± 8.5	1.38	-0.90	-5.6
28-00	0.966 ± 0.002	-59 ± 13	0.86	-0.97	-6.5
27-00	0.631 ± 0.002	-65 ± 15	9.1	-0.81	-10

$k_f = 2\pi/f_{\rm QPO}$; k_{obs} is the fitted slope of the relation between ϕ and Δf.

Reduced χ^2=$\chi^2/(5-2)$

Table 5. Model and Observation

Model	Prediction(E$\sim \Delta f$)	Observation	Reference
GDO	$\Delta f = 0$	no	Titarchuk 2000
ROOMs	$\Delta f \sim f(E)$	partial	Nowak & Wagoner 1993; Nowak 1994
AFIMs	$\Delta f \sim f(E)$	partial	Nowak 1994
DBM	$\Delta f \sim f(E)$	partial	Böttcher & Liang 1998, 1999; Hua et al. 1997

GDO=the global disk oscillation

ROOMs=the radial and orbital oscillation models

AFIMs=the accretion flow instability models

DBM=the drift blob model

partial=The model only explain partial observed phenomena.